














Improving population-level refractive error monitoring via mixture distributions

Timothy R. Fricke^{1,2,3}  | Lisa Keay¹  | Serge Resnikoff^{1,2}  | Nina Tahhan^{1,2}  |
Ornella Koumbo²  | Prakash Paudel^{1,2}  | Lauren N. Ayton^{3,4,5}  |
Alexis Ceecee Britten-Jones³  | Suhyun Kweon¹  | Josephine C. H. Li⁶ | Ling Lee¹  |
Peter Wagner¹  | Rebecca Weng²  | Boris Beranger^{7,8}  | Jake Olivier⁷ 

¹School of Optometry and Vision Science, University of New South Wales, Sydney, New South Wales, Australia

²Brien Holden Vision Institute, Sydney, New South Wales, Australia

³Department of Optometry and Vision Sciences, University of Melbourne, Melbourne, Victoria, Australia

⁴Department of Surgery (Ophthalmology), University of Melbourne, Melbourne, Victoria, Australia

⁵Centre for Eye Research Australia, Royal Victorian Eye and Ear Hospital, Melbourne, Victoria, Australia

⁶Australian College of Optometry, Carlton, Victoria, Australia

⁷School of Mathematics and Statistics, University of New South Wales, Sydney, New South Wales, Australia

⁸University of New South Wales Data Science Hub (uDASH), University of New South Wales, Sydney, New South Wales, Australia

Correspondence

Timothy R. Fricke, School of Optometry and Vision Science, University of New South Wales, Sydney, New South Wales 2052 Australia.

Email: t.fricke@unsw.edu.au

Funding information

Commonwealth Government of Australia; Brien Holden Vision Institute

Abstract

Introduction: Sampling and describing the distribution of refractive error in populations is critical to understanding eye care needs, refractive differences between groups and factors affecting refractive development. We investigated the ability of mixture models to describe refractive error distributions.

Methods: We used key informants to identify raw refractive error datasets and a systematic search strategy to identify published binned datasets of community-representative refractive error. Mixture models combine various component distributions via weighting to describe an observed distribution. We modelled raw refractive error data with a single-Gaussian (normal) distribution, mixtures of two to six Gaussian distributions and an additive model of an exponential and Gaussian (ex-Gaussian) distribution. We tested the relative fitting accuracy of each method via Bayesian Information Criterion (BIC) and then compared the ability of selected models to predict the observed prevalence of refractive error across a range of cut-points for both the raw and binned refractive data.

Results: We obtained large raw refractive error datasets from the United States and Korea. The ability of our models to fit the data improved significantly from a single-Gaussian to a two-Gaussian-component additive model and then remained stable with ≥ 3 -Gaussian-component mixture models. Means and standard deviations for BIC relative to 1 for the single-Gaussian model, where lower is better, were 0.89 ± 0.05 , 0.88 ± 0.06 , 0.89 ± 0.06 , 0.89 ± 0.06 and 0.90 ± 0.06 for two-, three-, four-, five- and six-Gaussian-component models, respectively, tested across US and Korean raw data grouped by age decade. Means and standard deviations for the difference between observed and model-based estimates of refractive error prevalence across a range of cut-points for the raw data were $-3.0\% \pm 6.3$, $0.5\% \pm 1.9$, $0.6\% \pm 1.5$ and $-1.8\% \pm 4.0$ for one-, two- and three-Gaussian-component and ex-Gaussian models, respectively.

Conclusions: Mixture models appear able to describe the population distribution of refractive error accurately, offering significant advantages over commonly quoted simple summary statistics such as mean, standard deviation and prevalence.

Presented in part at the International Myopia Conference in Rotterdam, Netherlands, 4–7 September 2022.

This is an open access article under the terms of the [Creative Commons Attribution](https://creativecommons.org/licenses/by/4.0/) License, which permits use, distribution and reproduction in any medium, provided the original work is properly cited.

© 2023 The Authors. *Ophthalmic and Physiological Optics* published by John Wiley & Sons Ltd on behalf of College of Optometrists.

KEYWORDS

epidemiology, hyperopia, myopia, population distribution, refractive error, statistical models

INTRODUCTION

Understanding the distribution of refractive error within a population promotes optimal eye care planning and delivery. Description of the refractive error distribution within population sub-groups additionally enables explorations of the refractive development effects of inherent variables such as age or sex, exposures such as screen time or sleep patterns and interventions such as mandated time spent outdoors or topical low-dose atropine. Description of the entire refractive error spectrum in a defined population can improve our understanding of the recent and dramatic increases in myopia prevalence seen in some communities¹ and enable work towards the World Health Organization's recommendation for integrated people-centred eye care.²

While the population distribution of neonatal refractive error is essentially normal,³ it is widely accepted that the distribution of refractive error develops a marked kurtosis giving an excess of emmetropia and skewness toward myopia.^{4,5} The emergence of both kurtosis and skewness in development can be explained by emmetropisation, in which ocular component growth is modulated by visual experience.^{4,5} The non-normality raises a question regarding the best way to describe the distribution. It has been standard to simply report refractive error prevalence at specific cut-points – for example, prevalence of myopia ≤ -0.50 D was 25%. Summary statistics are also common – for example, the mean spherical equivalent refraction (SER) was +0.12 D with a standard deviation of 1.93. Neither of these standard methods deals with the significant deviation from normality, potentially introducing inaccuracy and bias into any related analysis – for example, analysis of the influence of gender on myopia development. Efforts to understand the genetic and environmental mechanisms that determine refractive error may be obscured by the standard assumption of a normal distribution of refractive error in populations.

Single asymmetric distributions are difficult to apply to refractive error data, create difficulties comparing sub-groups using standard statistics and do not fit mechanistic concepts of refractive development.⁵ Mixture models, where component distributions are weighted and added to match the overall observed distribution, have been used in other fields and have potential to overcome these issues.⁶ Three studies have proposed mixture models for refractive data,^{5,7,8} but the proposals have not been widely adopted. Thorn⁷ and Flitcroft⁵ both focussed on the underlying mechanisms that might explain the success of describing refractive error distributions by adding two Gaussian (normal) components. Rozema et al.⁸ tested mixtures of up to six Gaussian components; however, their use of clinical data potentially introduces selection bias that clouds the generalisability of the model conclusions.

Key points

- Efforts to understand refractive error development and improve eye care access are hampered by the current standard of describing refractive error distributions by summary statistics such as mean, variance and/or prevalence.
- Two- and three-Gaussian-component mixture models can accurately describe accurately a wide variety of population-based refractive error distributions, and the ex-Gaussian additive model is a potentially useful alternative.
- Our recommended hierarchy for reporting refractive error population data: (i) repository of de-identified raw data or described by (ii) two- or three-component Gaussian mixture models, (iii) high-quality frequency distribution or (iv) mean, standard deviation, skewness and kurtosis.

No further investigation of the statistical accuracy, appropriateness or even use of mixture modelling to describe refractive distributions has been found. We explored mixture modelling options for describing population-based refractive distributions and compare the accuracy of the models identified.

METHODS

We identified publicly available raw datasets of refractive error in defined populations via literature search, web search and key informant advice. Our key informants were a range of experts with knowledge of refractive error epidemiology work around the world. We also identified published descriptions of refractive error distributions via a systematic search strategy.⁹ The published descriptions were most commonly graphs of density or frequency versus refractive error, which we digitised into binned datasets using the juicer package for R (rdr.io/github/mjlajeunesse/juicer/). Our systematic search strategy was built on key concepts of “refractive error”, “epidemiology” and “population”.⁹ Inclusion criteria were population-based sampling representative of clearly defined communities that quantified distance refractive error, clearly described the use (or not) of cycloplegic agents and reported sample size and participation rate. Exclusion criteria were self-reported refractive error and data from populations defined by disease state or condition.⁹

Mixture models combine component distributions via weighting to describe the overall distribution observed in epidemiologic research. Component distributions can take any form, but Gaussian (normal) components are appealing in the refractive case as they are the easiest to relate to underlying processes.^{5,7} A Gaussian mixture of K components has the form:

$$p(\theta) = \sum_{i=1}^K \pi_i \mathcal{N}(\mu_i, \sigma_i^2)$$

where $\mathcal{N}(\mu, \sigma^2)$ is a normal distribution with a mean of μ and a variance of σ^2 , π_i is the mixing weight for component i such that $\sum_{i=1}^K \pi_i = 1$ and θ is a vector of parameters to be estimated. The expectation-maximization (EM) algorithm is often used to find parameter estimates for the K mean/variance pairs (μ_i, σ_i^2) and $K-1$ mixing weights. A three-component Gaussian mixture, for example, has eight parameters that need to be estimated.

Additionally, we noted that adding an exponential component to a Gaussian component – that is, using the ex-Gaussian additive distribution – would generate the skewness and kurtosis common in population distributions of refractive error, potentially providing an accurate model.⁶ In its natural form, the ex-Gaussian additive distribution generates a positive skewness between zero and two. This level of positive skewness is commonly seen in populations with low levels of myopia, such as preschool-age Europeans. To generate the negative skewness common in populations from school age onwards, the sign of all SER details was reversed to enable the exponential component in the model to match the observed skewness.

The ex-Gaussian distribution is the sum of independent normal and exponential random variables, $Z = X + Y$, where X is a normal distribution $\mathcal{N}(\mu, \sigma^2)$ with mean of μ and variance of σ^2 and Y is an exponential distribution with mean λ . The three parameters μ , σ^2 and λ can be estimated from the sample mean, variance and skewness of the observed data.⁶ When skewness of the observed distribution was negative, myopia was denoted as “+” while hyperopia was denoted as “-” to enable the model to match the observed skewness.

We worked in the R environment ([r-project.org](https://www.r-project.org), and [rstudio.com](https://www.rstudio.com)), which provides adaptable options for fitting mixture distributions via numerous freely available packages including `gamlss`, `MixTools`, `FlexMix`, `FPC`, `Mclust`, `MixReg`, `MixDist` and `MixR`.^{10,11} `MixR` (github.com/GaryBAYLOR/mixR) was our first preference for fitting Gaussian-component mixture distributions because it is able to fit both raw and binned data and provides a wide range of fitting accuracy estimates, using the EM algorithm.¹² The Generalized Additive Models for Location, Scale and Shape (`GAMLSS`, gamlss.com) and `e1071` (cran.r-project.org/web/packages/e1071) packages were used to fit ex-Gaussian additive distributions.

The fitting algorithms and comparison statistics are more powerful when modelling raw data compared with binned data. So, the raw, all-ages datasets were modelled to compare fitting accuracy by visual observation, then by Bayesian information criterion (BIC). BIC is based on the likelihood function and is closely related to the Akaike Information Criterion but aims to prevent overfitting by penalising additional parameters in the model.¹³ The lowest BIC indicates the simplest, most accurate model.

The three models considered most useful by a combination of BIC and adaptability were then used to estimate the prevalence of refractive error at four representative refractive cut-points. The prevalence estimates from these three models, and from a single-Gaussian distribution as the accepted standard, were compared with observed data. This modelling and comparison were repeated with the all-ages raw data, the raw data divided into age decades and all binned datasets identified by our systematic search strategy. The four representative refractive cut-points were high myopia ($\text{SER} \leq -5.00 \text{ D}$), low myopia ($\text{SER} \leq -0.50 \text{ D}$), low hyperopia ($\text{SER} \geq +0.50 \text{ D}$) and high hyperopia ($\text{SER} \geq +4.00 \text{ D}$) when modelling the raw data. We matched these cut-points as closely as possible when modelling the binned data but adjusted each as required to maximise accuracy in response to the bin boundaries provided by the publications. That is, when the published bin boundaries did not match our representative cut-points, we used cut-points at the bin boundary closest to our representative cut-points. The combination of raw and binned datasets enabled assessment of the effect of data scarcity and diversity.

RESULTS

Identification of refractive error datasets

The National Health and Nutrition Surveys (NHANES) of the United States and South Korea were the two publicly available repositories of raw refractive error data found.^{14,15} Each is population-based, sampling multiple thousands of participants from across the respective countries, and each has been repeated multiple times. US NHANES samples all ages, with vision data available for those aged ≥ 12 -years from the 1971–1974, 1999–2000, 2001–2002, 2003–2004, 2005–2006 and 2007–2008 iterations of the survey. Korean NHANES samples all ages ≥ 5 years, with vision data available from the 2008, 2009, 2010, 2011 and 2012 iterations of the survey. NHANES does not use cycloplegia in either country. While the raw data are not nationally representative, nationally representative prevalence data can be derived via various adjustments based on demographic information such as age, sex, location, ethnicity and education. However, by their size, diversity and systematic sampling and testing, both NHANES datasets provide useful opportunities for testing refractive distribution modelling. We used data

from all available ages at the overlapping time point – the 2007–2008 US and 2008 Korean NHaNES.

An additional benefit of these datasets is the refractive diversity between South Korea and the United States. For example, myopia prevalence (≤ -0.50 D) in 20- to 29-year-old participants is 80.7% in South Korea compared with 47.7% in the United States. The diversity is a useful challenge for the models. Another benefit of NHaNES data is that participant numbers are large enough to be analysed by age decade, which reveals further diversity of refractive distributions due to age and/or cohort effects.

The raw refractive data obtained from both US (right eye data from 6034 participants) and Korean (right eye data from 4473 participants) NHaNES were in spherocylindrical form. We converted this to SER by adding the sphere and half the cylinder power.

Our systematic search strategy identified 665 published papers with population-based refractive error data from clearly defined communities. All 21 Global Burden of Disease study regions were represented by at least one study, demonstrating geographic spread.¹⁶ The highest number of studies were from the East Asia, Western Europe and North Africa-Middle East regions. Data collection occurred between 1917 and 2020, although most occurred between 1999 and 2019. Single datasets are sometimes used by multiple papers and this duplication has not been removed. With this caveat in mind, there were over 6000 reports of refractive error prevalence, with many papers reporting for multiple sub-groups within their sample and at several refractive cut-points.

From the 665 papers publishing population-based refractive error data, there were 168 quantifications of the refractive error spectrum providing significantly greater information than simply refractive error prevalence at one or a few refractive cut-points. Fifty-three of these provided density or frequency distributions of refractive error that could be arranged into ≥ 15 refractive bins with clear definitions and method descriptions. The average number of bins was 32, with a standard deviation of 21. There was no dataset duplication in the binned refractive distribution subset, so the duplication within the broader search strategy did not affect our analysis of refractive distribution fitting model accuracy. NHaNES data published as binned datasets were excluded from this analysis to avoid replication with our analysis of the NHaNES raw data. The binned refractive data included were from 12 Global Burden of Disease regions: East Africa,¹⁷ North Africa-Middle East,^{18,19} South Asia,^{20–22} East Asia,^{23–27} South East Asia,²⁸ Oceania,²⁹ Tropical Latin America,³⁰ North America High Income,^{31–33} Asia Pacific High Income,^{34–38} Australasia,^{4,39} Western Europe^{40–48} and Eastern Europe.⁴⁶ All were published in SER form. Some publications grouped participants by features such as age, sex or ethnicity and provided refractive distributions for each group; we accepted each as they posed differing challenges in terms of mean, variance, skew and kurtosis.

Model comparison part 1 – visual observation and fitting statistics

Multiple mixed Gaussian fits and an ex-Gaussian fit of the all-ages US and Korean NHaNES data are shown in [Figure 1](#). By visual observation, mixture distributions of two- to six-Gaussian components and the ex-Gaussian addition distribution all appear to describe the data better than the single-Gaussian model.

The BIC of each Gaussian mixture model fit of a refractive error distribution was recorded for the all-ages US NHaNES data, the all-ages Korean NHaNES data, seven separate age decade groups of the US NHaNES data and seven separate age decade groups of the Korean NHaNES data. The BIC consistently and significantly reduced, suggesting a better fit, from a single-Gaussian-component model to a two or more Gaussian-component mixture model. However, there were minimal differences between two- and six-component mixtures. Across the 16 data groupings, the BIC means and standard deviations relative to 1 for the single-Gaussian model were 0.89 ± 0.05 , 0.88 ± 0.06 , 0.89 ± 0.06 , 0.89 ± 0.06 and 0.90 ± 0.06 for two-, three-, four-, five- and six-Gaussian-component models, respectively. Remembering that BIC penalises model complexity, these results do not necessarily mean that the three-Gaussian-component models achieved a more accurate fit than the more complex models. However, balancing accuracy and simplicity, and avoiding overfitting, the two- or three-Gaussian-component models are preferred.

Model comparison part 2 – accuracy of refractive error prevalence estimates

Another way to compare the accuracy of refractive error distribution models is to test their ability to estimate the prevalence of refractive errors at particular cut-points. Based on the BIC results for model-fitting of the US and Korean raw data across all ages and within specific decades, we selected the two- and three-Gaussian-component mixture models to compare with a single-Gaussian model as the accepted standard, and the ex-Gaussian additive model as an interesting alternative. The “observed” prevalence at each cut-point was given by the raw data count, while “modelled” prevalence was the estimate derived from a model. We plotted the difference between the observed and modelled prevalence, against the observed prevalence, at each cut-point for the all-ages distributions and each age decade distribution of both the US and Korean NHaNES raw datasets. The results for each model are shown in [Figure 2](#).

From [Figure 2](#), means \pm standard deviations for observed prevalence minus estimated prevalence were $-3.0\% \pm 6.3\%$ for the single-Gaussian model, $0.5\% \pm 1.9\%$ for two-Gaussian, $0.6\% \pm 1.5\%$ for three-Gaussian and $-1.8\% \pm 4.0\%$ for ex-Gaussian model. Two- and three-Gaussian-component mixture models give model-estimated prevalence closer to the observed prevalence

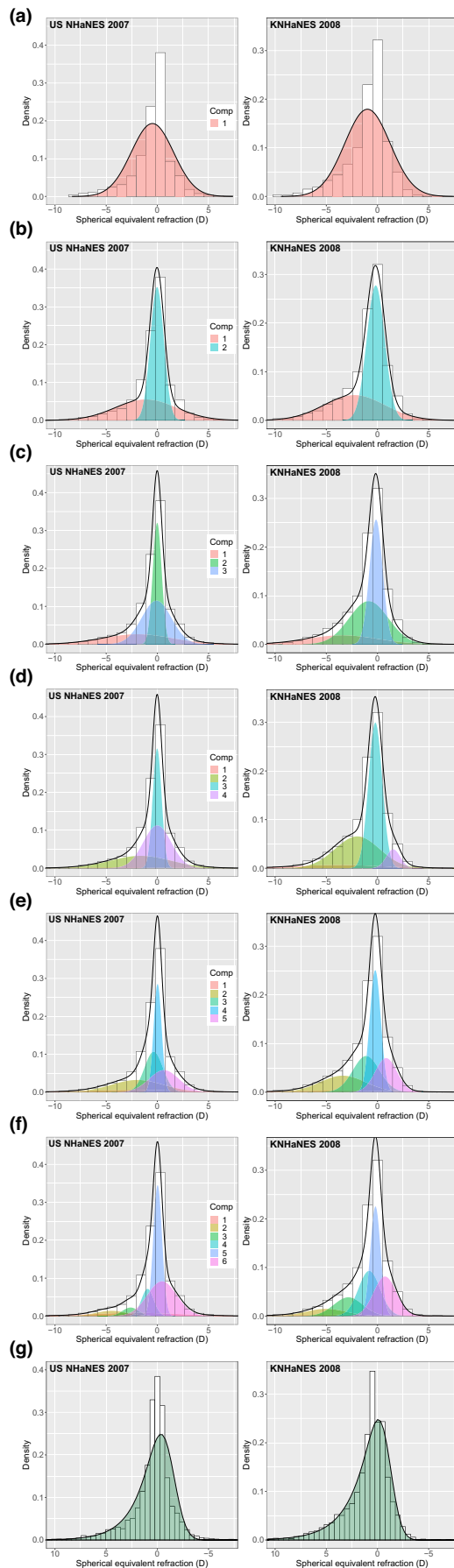


FIGURE 1 All-ages 2007–2008 US (left) and 2008 Korean (right) NHaNES data in white columns fitted with a one- to six-Gaussian mix (a–f, respectively, with components (Comp) as shaded areas and the mixture distribution shown as the black line) and an ex-Gaussian mix (g, with the shaded area showing the addition of the exponential and Gaussian components).

compared with the single-Gaussian or ex-Gaussian models. The ex-Gaussian model appears to have greater difficulty predicting the prevalence of low hyperopia than the prevalence of low myopia. However, it is worth noting that the ex-Gaussian is significantly more accurate than a single-Gaussian and can be used with less data input than multiple-Gaussian mixture models.

While Figure 2 shows that the US and Korean NHaNES datasets, grouped as all-ages and by age decade, provide a wide range of prevalence (0.1% to 81%) and skewness (−3.6 to −0.2) to challenge the models, it is still valuable to test model performance across a wider range of data types. To do this, we next used the high-quality binned refractive distributions in published papers identified by our systematic search strategy to estimate refractive prevalence at four refractive cut-points. These data varied greatly in participant age, ethnicity and location, as well as the number of bins into which the refractive distributions were divided. Figure 3 shows the accuracy of the single-Gaussian model was worse than each of the other models: means \pm standard deviations for each model were $-2.3\% \pm 7.3\%$ for single-Gaussian, $0.4\% \pm 3.5\%$ for two-Gaussian, $0.4\% \pm 3.3\%$ for three-Gaussian and $-1.2\% \pm 5.4\%$ for ex-Gaussian.

DISCUSSION

While there has been some debate between active versus passive modulation of refractive growth,⁴⁹ strong support has emerged over time for active emmetropisation driven by visual experience.^{4,5,50–52} After the major period of growth, development and emmetropisation has occurred, the complex population distribution of refractive errors that emerges is partly due to identifiable heterogeneity such as age, period, cohort, ethnicity, sex, education and urbanisation. However, even when participants are sub-grouped to isolate these factors, the distribution of refractive error in population-based samples remains non-normal, presumably due to variations in refractive genetics and visual experience. Perhaps the clearest published examples of this are from military conscription surveys.^{34,36}

Our analysis demonstrates the ability of multiple-Gaussian mixture models to describe the refractive development heterogeneity within a wide variety of population samples. It is tempting to imply biological meaning in the relationship – for example, that each Gaussian component of a mixture model represents a specific variation in refractive genetics or aligns with clinically meaningful groups like myopia, emmetropia and hyperopia, with the variance of each component representing the effects of the range of

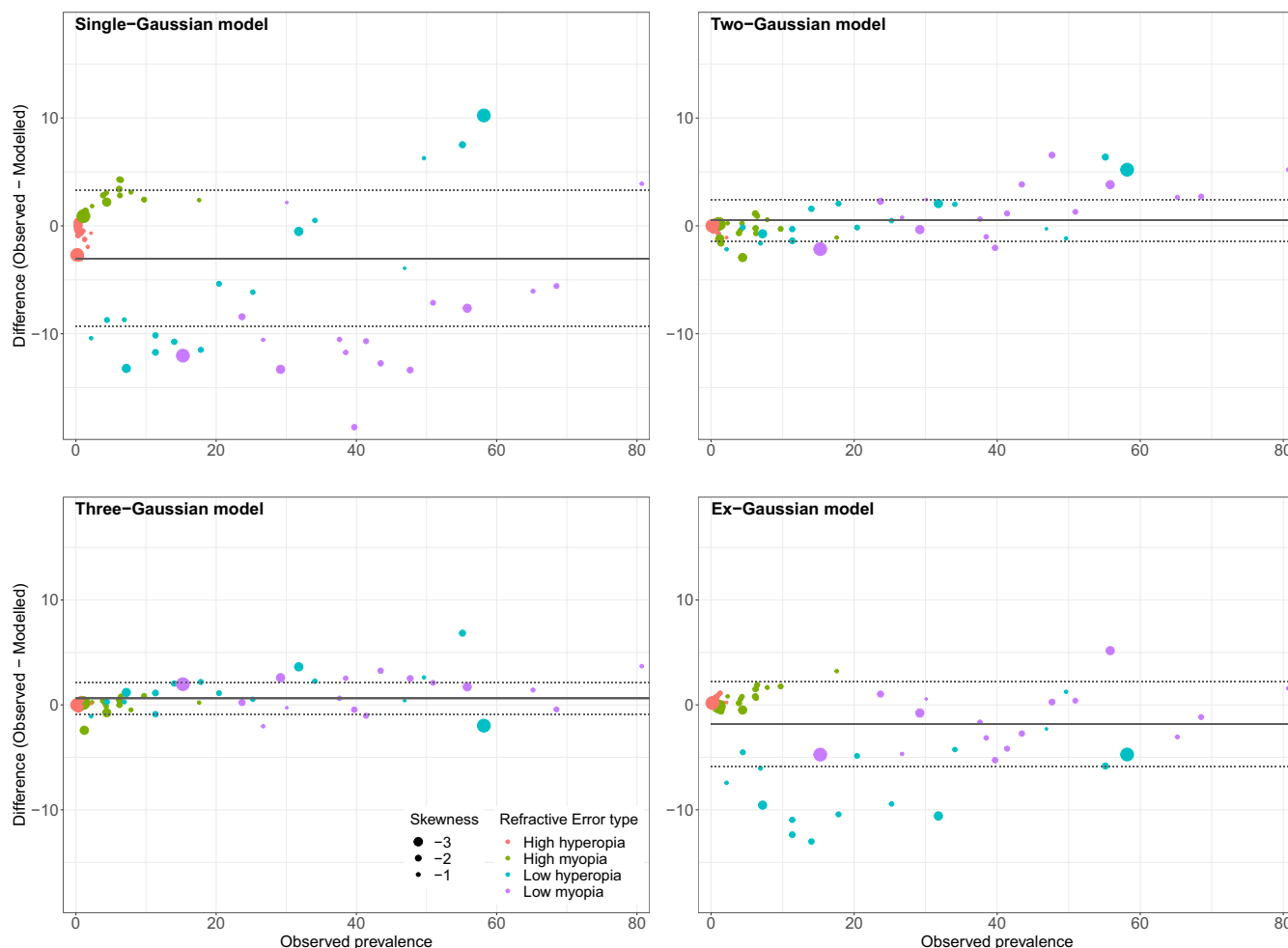


FIGURE 2 Comparison of prevalence from raw data counts (observed) with prevalence estimated by models (modelled), for US and Korean NHANES data divided into age decades. Data for high myopia ($\text{SER} \leq -5.00\text{D}$), low myopia ($\text{SER} \leq -0.50\text{D}$), low hyperopia ($\text{SER} \geq +0.50\text{D}$), high hyperopia ($\text{SER} \geq +4.00\text{D}$) are shown as different colours on each graph. The size of the data points shows the skewness in the observed distribution. Observed prevalence is compared with estimates from single-Gaussian (top left), two-Gaussian-component (top right), three-Gaussian-component (bottom left) and ex-Gaussian (bottom right) models. The solid, dark grey lines show the average difference between observed and modelled, with the dotted lines showing one standard deviation above (model under-estimated) and below (model over-estimated) the average.

visual experience. However, our analysis does not provide any proof of the underlying mechanism, only that mixed-Gaussian models are a reasonably accurate way to describe observed distributions of refractive error. Even so, the existence of a plausible underlying mechanism is reassuring when considering the use of mixture models in measuring and understanding distributions of refractive error.

“All models are wrong” is a common statistics aphorism⁵³ but can less nihilistically be expanded to “All models are wrong, but some are useful”. We have argued that there is a need to better understand the distribution of refractive errors in populations, and we have shown that mixture modelling is, while not perfect, a substantial improvement on the currently accepted standard of a single-Gaussian model. Although multiple-Gaussian mixtures outperform the ex-Gaussian additive model when raw data are available, the ex-Gaussian model still appears useful where there is limited binned distribution data and particularly when only summary statistics are available for a particular population. It is

important to understand the imperfections of the models but that each can be useful for predicting the prevalence of refractive error at standardised refractive cut-points.

A major strength of our analysis is that all the refractive data, both raw and binned, were population-based. This overcomes the possible bias of clinical data such as that used by Rozema et al.⁸ Even so, it is worth noting that Rozema et al.⁸ came to similar conclusions from their analysis of clinical refractive data. Similarly, our findings appear consistently robust across the widely diverse range of population-based data we obtained. One limitation in our analysis is that by analysing SER, we have averaged out some additional complexities of refractive error such as astigmatism. A clear understanding of astigmatism is critical in planning and delivering integrated people-centred eye care, so methods of taking it into account in modelling are also needed.

The ability to analyse and compare data across different studies accurately will facilitate progress in understanding

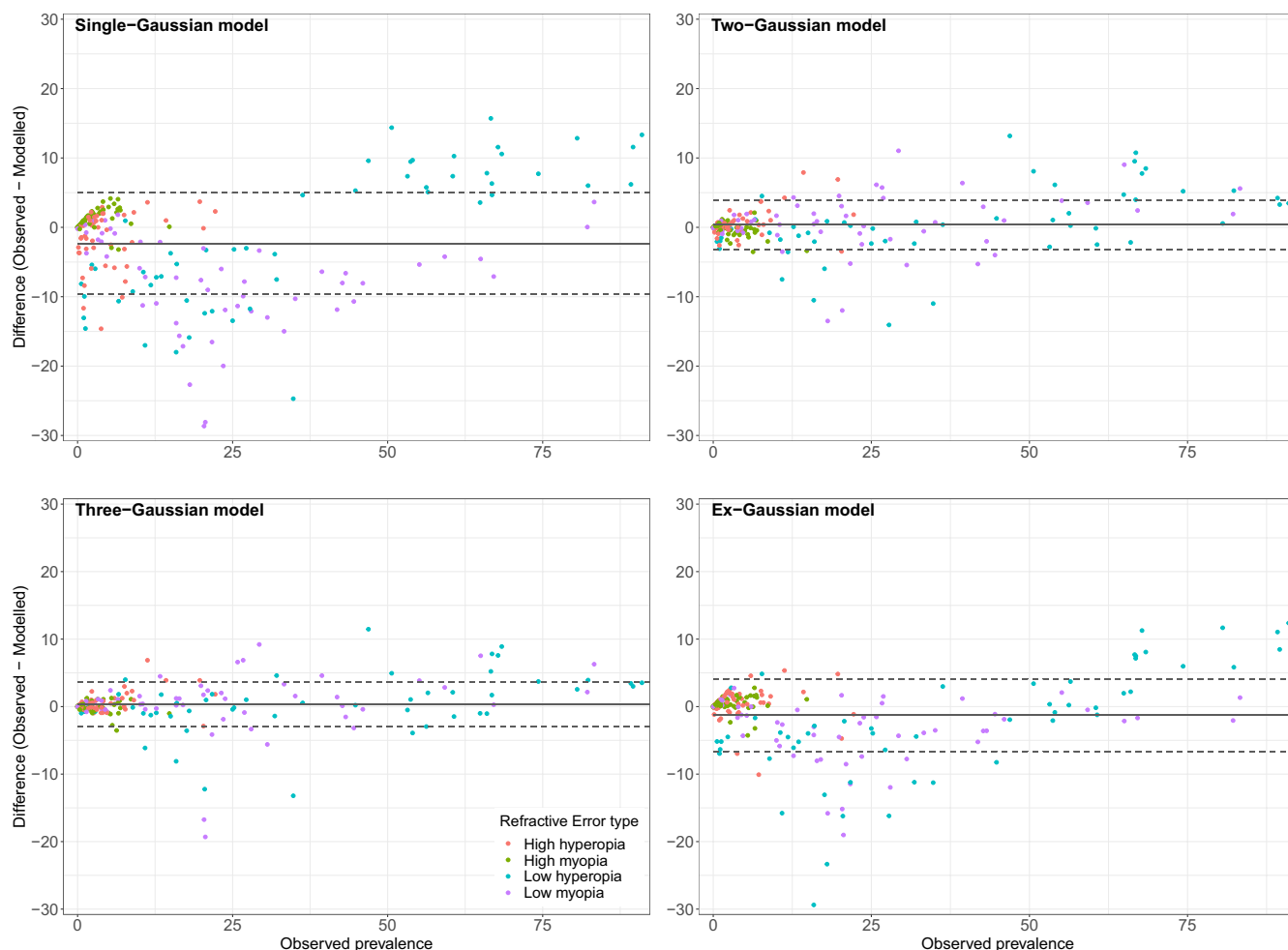


FIGURE 3 Comparison of published prevalence (observed) with prevalence estimated by models (modelled), for 53 published refractive error distributions provided as density or frequency in varying numbers of bins. There are four observed-modelled comparison points on each graph from each distribution – one each for high myopia, low myopia, low hyperopia and high hyperopia. Observed prevalence is compared with estimates from single-Gaussian (top left), two-Gaussian-component (top right), three-Gaussian-component (bottom left) and ex-Gaussian (bottom right) models. The solid dark grey lines show the average difference between observed and modelled, with the dotted lines showing one standard deviation above (model under-estimated) and below (model over-estimated) the average.

refractive error development and improving eye care access and delivery. The systematic search strategy used here suggests most publications simply report refractive error prevalence at non-standardised cut-points, which are difficult to compare. We have also shown that it is inaccurate, and potentially biased and misleading, to assume normality in grouped comparisons. As such, it seems worth considering a hierarchy of data sharing and description that would maximise the power and potential of meta-analyses, while recognising that the first priority is not always possible. Our recommended hierarchy would be to publish:

1. Full datasets of de-identified participant-level data in open-access repositories such as those provided by the US and Korean NHaNES.^{14,15} This would be in line with the United Nations Educational, Scientific and Cultural Organization's (UNESCO's) 2021 Recommendation on Open Science⁵⁴ and new US government policy regarding publicly funded research.⁵⁵

2. A two- or three-component Gaussian mixture model describing the refractive error distribution/s, which our results demonstrate to be accurate in a variety of populations. For example, as per our Methods section, a three-component Gaussian mixture model can be specified by three mean/variance pairs and two mixing weights.
3. A high-quality frequency distribution, or binned datasets of 25 bins or more, describing the refractive error distribution/s. These generally need to be modelled (e.g., by multiple-Gaussian or ex-Gaussian mixture models) to be used accurately in meta-analyses.
4. The mean, standard deviation, skewness and kurtosis of the refractive error distribution/s, which would enable modelling using the ex-Gaussian additive distribution.

Each of the four levels of this hierarchy offers significant advantages over currently commonly quoted simple summary statistics such as mean, standard deviation and prevalence at specific cut-points.

AUTHOR CONTRIBUTIONS

Timothy R. Fricke: Conceptualization (lead); data curation (lead); formal analysis (lead); funding acquisition (equal); investigation (lead); methodology (lead); project administration (lead); resources (equal); software (equal); validation (lead); visualization (lead); writing – original draft (lead); writing – review and editing (lead). **Lisa Keay:** Conceptualization (supporting); data curation (supporting); formal analysis (supporting); funding acquisition (equal); investigation (supporting); methodology (supporting); project administration (supporting); resources (equal); supervision (equal); visualization (supporting); writing – review and editing (supporting). **Serge Resnikoff:** Conceptualization (supporting); formal analysis (supporting); supervision (supporting); writing – review and editing (supporting). **Nina Tahhan:** Conceptualization (supporting); data curation (supporting); formal analysis (supporting); investigation (supporting); methodology (supporting); supervision (supporting); visualization (supporting); writing – review and editing (supporting). **Ornella Koumbo:** Data curation (supporting). **Prakash Paudel:** Data curation (supporting); writing – review and editing (supporting). **Lauren N. Ayton:** Data curation (supporting). **Alexis Ceecee Britten-Jones:** Data curation (supporting); writing – review and editing (supporting). **Suhyun Kweon:** Data curation (supporting). **Josephine C. H. Li:** Data curation (supporting). **Ling Lee:** Data curation (supporting); writing – review and editing (supporting). **Peter Wagner:** Data curation (supporting). **Rebecca Weng:** Data curation (supporting). **Boris Beranger:** Formal analysis (supporting). **Jake Olivier:** Conceptualization (supporting); formal analysis (supporting); methodology (supporting); supervision (supporting); visualization (supporting); writing – review and editing (supporting).




FUNDING INFORMATION

This work was supported by an Australian Government Research Training Program scholarship and a public health grant from the Brien Holden Vision Institute (BHVI), Sydney, Australia.

CONFLICT OF INTEREST STATEMENT

No conflict of interest is declared.

ORCID

Timothy R. Fricke  <https://orcid.org/0000-0001-8087-6835>
 Lisa Keay  <https://orcid.org/0000-0003-2215-0678>
 Serge Resnikoff  <https://orcid.org/0000-0002-5866-4446>
 Nina Tahhan  <https://orcid.org/0000-0002-8856-2483>
 Ornella Koumbo  <https://orcid.org/0000-0002-8018-7711>
 Prakash Paudel  <https://orcid.org/0000-0002-9809-9672>
 Lauren N. Ayton  <https://orcid.org/0000-0001-9907-084X>
 Alexis Ceecee Britten-Jones  <https://orcid.org/0000-0002-1101-2870>
 Suhyun Kweon  <https://orcid.org/0000-0002-8806-5348>
 Ling Lee  <https://orcid.org/0000-0003-0908-7280>
 Peter Wagner  <https://orcid.org/0000-0001-7835-3357>

Rebecca Weng  <https://orcid.org/0000-0001-8458-4979>

Boris Beranger  <https://orcid.org/0000-0002-7944-3925>

Jake Olivier  <https://orcid.org/0000-0002-3144-4507>

REFERENCES

- Holden BA, Fricke TR, Wilson DA, Jong M, Naidoo KS, Sankaridurg P, et al. Global prevalence of myopia and high myopia and temporal trends from 2000 through 2050. *Ophthalmology*. 2016;123:1036–42.
- World Health Organization. World report on vision. Geneva: World Health Organization; 2019.
- Mutti DO, Mitchell GL, Jones LA, Friedman NE, Frane SL, Lin WK, et al. Axial growth and changes in lenticular and corneal power during emmetropization in infants. *Invest Ophthalmol Vis Sci*. 2005;46:3074–80.
- Ojaimi E, Rose KA, Morgan IG, Smith W, Martin FJ, Kifley A, et al. Distribution of ocular biometric parameters and refraction in a population-based study of Australian children. *Invest Ophthalmol Vis Sci*. 2005;46:2748–54.
- Flitcroft DI. Is myopia a failure of homeostasis? *Exp Eye Res*. 2013;114:16–24.
- Olivier J, Norberg MM. Positively skewed data: revisiting the Box-cox power transformation. *Int J Psychol Res*. 2010;3:69–78.
- Thorn F. Mathematical models of refractive distributions suggest different underlying mechanisms in Chinese and Western myopes. *Invest Ophthalmol Vis Sci*. 2007;48:ARVO E-abstract 1025.
- Rozema JJ, Tassignon MJ, for EVICR.net, Project Gullstrand Study Group. The bigaussian nature of ocular biometry. *Optom Vis Sci*. 2014;91:713–22.
- Fricke TR, Keay L, Resnikoff S, Tahhan N. Global estimates of distance refractive errors and associated vision impairment. *Prospero*; 2021. Available from: https://www.crdyork.ac.uk/prospero/display_record.php?ID=CRD42021267350. Accessed 12 Sep 2022.
- R Core Team. R: a language and environment for statistical computing. Vienna, Austria: R Foundation for Statistical Computing; 2020.
- RStudio Team. RStudio: integrated development for R. Boston, MA: RStudio PBC; 2020.
- Yu Y. MixR: an R package for finite mixture modeling for both raw and binned data. *J Open Source Software*. 2022;7:4031. <https://doi.org/10.21105/joss.04031>
- Schwarz G. Estimating the dimension of a model. *Ann Stat*. 1978;6:461–4.
- Centers for Disease Control and Prevention. National Health and Nutrition Examination Survey (NHANES). CDC; 2022. Available from: <https://www.cdc.gov/nchs/nhanes/Default.aspx>. Accessed 18 Aug 2022.
- Korea Disease Control and Prevention Agency. Korea National Health and nutrition examination survey (KNHANES). KDCA; 2022. Available from: <https://www.knhanes.kdca.go.kr/knhanes/eng/index.do>. Accessed 18 Aug 2022.
- Bourne RR, Stevens GA, White RA, Smith JL, Flaxman SR, Price H, et al. Causes of vision loss worldwide, 1990–2010: a systematic analysis. *Lancet Glob Health*. 2013;1:e339–49.
- Lewallen S, Lowdon R, Courtright P, Mehl GL. A population-based survey of the prevalence of refractive error in Malawi. *Ophthalmic Epidemiol*. 1995;2:145–9.
- Hashemi H, Rezvan F, Ostadimoghaddam H, Abdollahi M, Hashemi M, Khabazkhoob M. High prevalence of refractive errors in a rural population: ‘Nooravaran Salamat’ Mobile Eye Clinic experience. *Clin Experiment Ophthalmol*. 2013;41:635–43.
- Hashemi H, Rezvan F, Beiranvand A, Papi OA, Hoseini Yazdi H, Ostadimoghaddam H, et al. Prevalence of refractive errors among high school students in western Iran. *J Ophthalmic Vis Res*. 2014;9:232–9.
- Murthy GV, Gupta SK, Ellwein LB, Muñoz SR, Pokharel GP, Sanga L, et al. Refractive error in children in an urban population in New Delhi. *Invest Ophthalmol Vis Sci*. 2002;43:623–31.

21. Shah SP, Jadoon MZ, Dineen B, Bourne RRA, Johnson GJ, Gilbert CE, et al. Refractive errors in the adult Pakistani population: the National Blindness and Visual Impairment Survey. *Ophthalmic Epidemiol.* 2008;15:183–90.
22. Nangia V, Jonas JB, Sinha A, Matin A, Kulkarni M. Refractive error in Central India: the Central India eye and medical study. *Ophthalmology.* 2010;117:693–9.
23. Liang YB, Wong TY, Sun LP, Tao QS, Wang JJ, Yang XH, et al. Refractive errors in a rural Chinese adult population. The Handan eye study. *Ophthalmology.* 2009;116:2119–27.
24. Peng L, Gao L, Zheng Y, Dai Y, Xie Q. Refractive errors and visual impairment among children and adolescents in southernmost China. *BMC Ophthalmol.* 2021;21:227. <https://doi.org/10.1186/s12886-021-01993-5>
25. Liu S, Ye S, Xi W, Zhang X. Electronic devices and myopic refraction among children aged 6–14 years in urban areas of Tianjin, China. *Ophthalmic Physiol Opt.* 2019;39:282–93.
26. Xu C, Pan C, Zhao C, Bi M, Ma Q, Cheng J, et al. Prevalence and risk factors for myopia in older adult east Chinese population. *BMC Ophthalmol.* 2017;17:191. <https://doi.org/10.1186/s12886-017-0574-4>
27. Pi LH, Chen L, Liu Q, Ke N, Fang J, Zhang S, et al. Refractive status and prevalence of refractive errors in suburban school-age children. *Int J Med Sci.* 2010;7:342–53.
28. Gupta A, Casson RJ, Newland HS, Muecke J, Landers J, Selva D, et al. Prevalence of refractive error in rural Myanmar: the Meiktila eye study. *Ophthalmology.* 2008;115:26–32.
29. Grosvenor T. Myopia in Melanesian school children in Vanuatu. *Acta Ophthalmol Suppl.* 1988;185:24–8.
30. Yotsukura E, Torii H, Ozawa H, Hida RY, Shiraishi T, Corso Teixeira I, et al. Axial length and prevalence of myopia among schoolchildren in the equatorial region of Brazil. *J Clin Med.* 2021;10:115. <https://doi.org/10.3390/jcm10010115>
31. Katz J, Tielsch JM, Sommer A. Prevalence and risk factors for refractive errors in an adult inner city population. *Invest Ophthalmol Vis Sci.* 1997;38:334–40.
32. Johnson GJ, Matthews A, Perkins ES. Survey of ophthalmic conditions in a Labrador community. I. Refractive errors. *Br J Ophthalmol.* 1979;63:440–8.
33. Brody BL, Roch-Leveq AC, Klonoff-Cohen HS, Brown SI. Refractive errors in low-income preschoolers. *Ophthalmic Epidemiol.* 2007;14:223–9.
34. Lee JH, Jee D, Kwon JW, Lee WK. Prevalence and risk factors for myopia in a rural Korean population. *Invest Ophthalmol Vis Sci.* 2013;54:5466–70.
35. Sawada A, Tomidokoro A, Araie M, Iwase A, Yamamoto T, Tajimi Study Group. Refractive errors in an elderly Japanese population: the Tajimi study. *Ophthalmology.* 2008;115:363–70.
36. Wu H-M, Seet B, Yap EP-H, Saw SM, Lim TH, Chia KS. Does education explain ethnic differences in myopia prevalence? A population-based study of young adult males in Singapore. *Optom Vis Sci.* 2001;78:234–9.
37. Pan CW, Wong TY, Lavanya R, Wu RY, Zheng YF, Lin XY, et al. Prevalence and risk factors for refractive errors in Indians: the Singapore Indian eye study (SINDI). *Invest Ophthalmol Vis Sci.* 2011;52:3166–73.
38. Watanabe S, Yamashita T, Ohba N. A longitudinal study of cycloplegic refraction in a cohort of 350 Japanese schoolchildren. Cycloplegic refraction. *Ophthalmic Physiol Opt.* 1999;19:22–9.
39. Junghans B, Kiely PM, Crewther DP, Crewther SG. Referral rates for a functional vision screening among a large cosmopolitan sample of Australian children. *Ophthalmic Physiol Opt.* 2002;22:10–25.
40. Wolfram C, Hohn R, Kottler U, Wild P, Blettner M, Bühren J, et al. Prevalence of refractive errors in the European adult population: the Gutenberg health study (GHS). *Br J Ophthalmol.* 2014;98:857–61.
41. Hyams SW, Pokotilo E, Shkurko G. Prevalence of refractive errors in adults over 40: a survey of 8102 eyes. *Br J Ophthalmol.* 1977;61:428–32.
42. Tideman JW, Parssinen O, Haarman AEG, Khawaja AP, Wedenoja J, Williams KM, et al. Evaluation of shared genetic susceptibility to high and low myopia and hyperopia. *JAMA Ophthalmol.* 2021;139:601–9.
43. Hagen LA, Gjelle JVB, Arnegard S, Pedersen HR, Gilson SJ, Baraas RC. Prevalence and possible factors of myopia in Norwegian adolescents. *Sci Rep.* 2018;8:13479. <https://doi.org/10.1038/s41598-018-31790-y>
44. Olsen T, Arnarsson A, Sasaki H, Sasaki K, Jonasson F. On the ocular refractive components: the Reykjavik eye study. *Acta Ophthalmol Scand.* 2007;85:361–6.
45. Norn M. Myopia among the Inuit population of East Greenland. Longitudinal study 1950–1994. *Acta Ophthalmol Scand.* 1997;75:723–5.
46. Williams KM, Verhoeven VJ, Cumberland P, Bertelsen G, Wolfram C, Buitendijk GH, et al. Prevalence of refractive error in Europe: the European eye epidemiology (E(3)) consortium. *Eur J Epidemiol.* 2015;30:305–15.
47. Harrington SC, Stack J, Saunders K, O'Dwyer V. Refractive error and visual impairment in Ireland schoolchildren. *Br J Ophthalmol.* 2019;103:1112–8.
48. Atkinson J, Braddick O, Nardini M, Anker S. Infant hyperopia: detection, distribution, changes and correlates: outcomes from the Cambridge infant screening programs. *Optom Vis Sci.* 2007;84:84–96.
49. Hofstetter HW. Emmetropization – biological process or mathematical artifact? *Am J Optom Arch Am Acad Optom.* 1969;46:447–50.
50. Wildsoet CF. Active emmetropization – evidence for its existence and ramifications for clinical practice. *Ophthalmic Physiol Opt.* 1997;17:279–90.
51. Sorsby A, Benjamin B, Sheridan M, Stone J, Leary GA. Refraction and its components during the growth of the eye from the age of three. *Memo Med Res Counc.* 1961;301:1–67.
52. Sorsby A, Leary GA. A longitudinal study of refraction and its components during growth. *Spec Rep Ser Med Res Counc.* 1969;309:1–41.
53. Box GEP. Science and statistics. *J Am Stat Assoc.* 1976;71:791–9.
54. United Nations Educational Scientific and Cultural Organization. UNESCO recommendation on open science. UNESCO; 2021. Available from: <https://www.unesco.org/en/natural-sciences/open-science>. Accessed 30 Aug 2022.
55. Marcum C, Donohue R. Breakthroughs for all: delivering equitable access to America's research. Washington, DC: The White House; 2022.

How to cite this article: Fricke TR, Keay L, Resnikoff S, Tahhan N, Koumbo O, Paudel P, et al. Improving population-level refractive error monitoring via mixture distributions. *Ophthalmic Physiol Opt.* 2023;43:445–453. <https://doi.org/10.1111/opo.13105>